Low-dose dioxin exposure during pregnancy and lactation increases susceptibility to diet-induced diabetes in dams

Myriam P Hoyeck[1], Rayanna C Merhi[1], Hannah Blair[1], C Duncan Spencer[2], Mikayla A Payant[2], Diana I Martin Alfonso[2], Melody Zhang[1], Melissa J Chee[2], Jennifer E Bruin[1]*

[1]Department of Biology & Institute of Biochemistry, Carleton University, Ottawa, ON, Canada
[2]Department of Neuroscience, Carleton University, Ottawa, ON, Canada

* Address correspondence to:
Dr. Jennifer Bruin
1125 Colonel By Drive
Ottawa, ON K1S 5B6
T: 613-520-2600 x3656
jenny.bruin@carleton.ca

Abstract

Aim/hypothesis:
Persistent organic pollutants have consistently been associated with increased diabetes risk in humans. However, very few studies have assessed the risk of chronic low-dose exposure to pollutants during pregnancy. We investigated the short- and long-term impact of chronic low-dose dioxin exposure during pregnancy and lactation on glucose homeostasis and beta cell function in female mice, including their response to a metabolic stressor later in life.
Methods:
Female mice were injected with either corn oil (CO; vehicle control) or 20 ng/kg/d TCDD 2x/week throughout mating, pregnancy, and lactation, and then tracked for 6-10 weeks after chemical exposure stopped. A subset of CO- and TCDD-exposed dams were then transferred to a 45% high fat diet (HFD) or remained on standard chow diet for an additional 11 weeks to assess long-term effects of TCDD on adaptability to a metabolic stressor.
Results:
Dioxin-exposed dams were hypoglycemic at birth but otherwise had normal glucose homeostasis during and post-dioxin exposure. However, dioxin-exposed dams were modestly heavier than controls starting 5 weeks after the last dioxin injection, and their weight gain accelerated after transitioning to a HFD. Dioxin-exposed dams fed HFD also had accelerated onset of hyperglycemia, dysregulated insulin secretion, reduced islet size, increased $MAFA^-$ beta cells, and impaired proinsulin processing compared to control dams on HFD.
Conclusions/interpretations:
Our study suggests that chronic low-dose dioxin exposure during pregnancy may contribute to the rapid rise in obesity and diabetes incidence seen worldwide.

Keywords

Beta cells, diabetes, dioxin, insulin, metabolic plasticity, obesity, pollution, pregnancy

Abbreviations

AhR	Aryl hydrocarbon receptor
CO	Corn Oil
Cyp	Cytochrome P450
Cyp1a1	Cytochrome P450 1A1
Cyp1a2	Cytochrome P450 1A2
GDM	Gestational diabetes mellitus
GSIS	Glucose stimulated insulin secretion
GTT	Glucose tolerance test
HFD	High fat diet
ITT	Insulin tolerance test
POPs	Persistent Organic Pollutants
TCDD	2,3,7,8-tetrachlorodibenzo-*p*-dioxin

Introduction

Diabetes is a global health concern, with incidence rates tripling over the past 20 years [1]. This disease is characterised by chronic hyperglycemia, defects in insulin secretion from pancreatic beta cells, and impaired peripheral insulin action [2]. Type 2 diabetes accounts for 90-95% of all diabetes cases and is strongly associated with genetic and lifestyle determinants (e.g. physical inactivity, poor diet, and obesity). Interestingly, epidemiological studies consistently report significant associations between exposure to persistent organic pollutant (POPs) and increased diabetes incidence in humans [3, 4].

POPs are mainly lipophilic chemicals that resist degradation, leading to widespread environmental dispersion and biomagnification [5]. Dioxins and dioxin-like compounds are a broad class of POPs that induce cellular toxicity through persistent activation of the aryl hydrocarbon receptor (AhR), and upregulation of AhR-target genes including cytochrome P450 *(Cyp)1a1* and *Cyp1a2* [6]. CYP enzymes are phase I xenobiotic metabolism enzymes that play an essential role in the oxidation of xenobiotic compounds for subsequent excretion from the body. However, this process generates highly reactive intermediate metabolites that can sometimes cause oxidative stress and DNA/protein damage [7]. Although the pancreas is not traditionally considered a target organ for environmental chemicals, we showed that CYP1A enzymes are inducible and functional in human and mouse pancreatic islets [8]. These data suggest that dioxins reach the endocrine pancreas *in vivo*, which may impact beta cell function and survival.

Human studies consistently report a positive association between serum concentrations of dioxin/dioxin-like chemicals with insulin-resistance [9–11] and increased diabetes incidence [12–17]. There is also growing evidence suggesting that POPs may impair beta cell function [8, 18–21]. In fact, our lab has shown that direct exposure of mouse and human islets to the highly persistent dioxin 2,3,7,8-tetrachlorodibenzo-*p*-dioxin (TCDD) for 48-hours *ex vivo* led to a significant reduction in glucose-induced insulin secretion [8]. In addition, a single high-dose injection of TCDD (20 µg/kg) *in vivo* reduced plasma insulin levels for up to 6 weeks in male and female mice [18]. TCDD-exposed males also displayed modest fasting hypoglycemia for ~4 weeks post-injection, increased insulin sensitivity, decreased beta cell area, and increased delta cell area. In contrast, TCDD-exposed females became transiently glucose intolerant 4 weeks after the single high-dose TCDD injection [18]. These results suggest that pollutants may increase diabetes risk by altering beta cell function and/or islet composition in a sex-dependent manner.

Most epidemiological studies investigating the association between POPs and diabetes have focused on adult populations subjected to acute dioxin exposure (e.g. war veterans, occupational workers, and victims of chemical disasters) [13–15, 22], and chronic exposure in at-risk populations [16, 17, 23]. However, very few studies have assessed the risk of chronic low-dose POP exposure during pregnancy. Pregnancy is a unique period of metabolic plasticity in females, during which beta cells proliferate and increase insulin secretion to accommodate for changes in nutritional needs [24–27]. Failure to compensate for these changes can lead to hyperglycemia, gestational diabetes mellitus (GDM), and long-term metabolic complications in the mothers and their offspring [28]. The limited number of epidemiological studies that assessed the association between chronic POP exposure and GDM have reported inconsistent results, with some studies showing a positive association between POP serum levels and GDM [29–32] and others showing

no association [32–34]. In addition, these are all cross-sectional studies and therefore do not provide information about the timing of events and cannot rule out the possibility of reverse causality (i.e. whether POPs increased GDM risk, or whether GDM increased serum POP accumulation). Lastly, long-term tracking is not possible with cross-sectional epidemiological studies.

The purpose of our study was to determine whether chronic low-dose TCDD exposure during pregnancy and lactation impacts pancreatic beta cell plasticity or glucose homeostasis during this critical period of metabolic stress in female mice. Secondly, we investigated whether there are lasting metabolic consequences of transient TCDD exposure during pregnancy and lactation on dams, including their ability to adapt to high fat diet (HFD) feeding later in life.

Research Design and Methods

Animals

C57BL/6 mice, 5-8 week old (Charles River; Raleigh, NC, USA), were maintained on a 12-hour light/dark cycle throughout the study and received *ad libitum* access to standard rodent chow (Harlan Laboratories, Teklad Diet #2018, Madison, WI). All experiments were approved by the Carleton University Animal Care Committee and carried out in accordance with the Canadian Council on Animal Care guidelines. Prior to beginning experimental protocols, animals were randomly assigned to treatment groups and matched for body weight and blood glucose to ensure that these variables were consistent between groups.

Cohort 1 (Fig. S1-S2): As outlined in **Fig. 1A**, female mice received subcutaneous injections (s.c.) of corn oil (CO) (25 ml/kg, vehicle control; n = 6) (#C8267-2.5L, Sigma-Aldrich, St Louise, MO, USA) or a low-dose of TCDD (20 ng/kg/d; n = 6) (Sigma Aldrich, # 48599) 2x/week starting one week prior to pairing with male mice and lasting throughout mating and pregnancy. All mice were euthanized at postnatal day 1 (P1). Whole pancreas was harvested and stored in RNAlater (#76106, Qiagen, Hilden, Germany) for quantitative real-time PCR (qPCR) analysis or 4% paraformaldehyde (PFA) (#AAJ19943K2, Thermo Fisher Scientific, Waltham, MA, USA) for 24 hrs, followed by long-term storage in 70% EtOH for histological analysis.

Cohort 2 (Fig. 1-7, S3-S4): As outlined in **Fig. 1A**, female mice received s.c. injections of corn oil (25 ml/kg, vehicle control; n = 12) or a low-dose of TCDD (20 ng/kg/d; n = 14) 2x/week starting one week prior to pairing with male mice and lasting throughout mating, pregnancy, and lactation ("TCDD Injections" window: weeks 0-7 of the study). Metabolic assessments were performed on chow-fed dams for 6 to 10 weeks following the last TCDD exposure ("Post-TCDD" window: weeks 7-17 of the study). This range reflects differences in the duration of mating, with a 4 week difference between the first and last pregnancies. As outlined in **Fig. 1A**, a subset of CO- and TCDD-exposed dams were then transferred to a 45% high fat diet (Research Diets D12451, New Brunswick, NJ) or remained on a standard chow diet (n=4-5 per group) for an additional 11 weeks ("Metabolic Challenge" window). Whole pancreas, liver, perirenal fat, and placenta were harvested from a subset of mice at approximately day 15.5 of pregnancy (GD15.5) (n=3-4/group). Whole pancreas and hypothalamic brain tissue were collected at week 11 of the metabolic challenge (n=4-5/group). Tissues were stored in RNAlater or 4% PFA.

Metabolic Assessment

All metabolic analyses were performed in conscious, restrained mice, and blood samples were collected via the saphenous vein using heparinized microhematocrit tubes. Blood glucose levels were measured using a handheld glucometer (Lifescan; Burnaby; Canada)

Body weight and blood glucose were measured weekly or 2x/week following a 4-hour morning fast. Saphenous blood was collected at GD15.5, P1, lactation (P14), and weaning (P21) following a 4-hour morning fast to measure plasma insulin levels by ELISA (#80-INSMSU-E01, ALPCO, Salem, NH, USA). For all metabolic tests, time 0 indicates the blood sample collected prior to administration of glucose or insulin. For glucose tolerance tests (GTTs), mice received an intraperitoneal (i.p.) bolus of glucose (2 g/kg) following a 4-hour morning fast. Blood samples were collected at times 0, 15, and 30 minutes for measuring plasma insulin levels by ELISA. For insulin tolerance tests (ITTs), mice received an i.p. bolus of insulin (0.7 IU/kg: **Fig. 2F**, **4D** and **S4B**; 1.0 IU/kg: **Fig. 4B**) (Novolin ge Toronto; Novo Nordisk Canada, #02024233) following a 4-hour morning fast. Cardiac blood was collected at week 11 of the metabolic challenge for measuring random-fed plasma leptin levels (#90030, Crystal Chem, Elk Grove Village, IL, USA), proinsulin levels (ALPCO, #80-PINMS-E01), and insulin levels (ALPCO, #80-INSMSU-E01) by ELISA.

Food Intake Analysis

Food intake was assessed mid-pregnancy, lactation (P14), and at week 7 of the metabolic challenge. All dams were singly housed for this experiment. Dams were transferred to a clean cage and the amount of food in their feeding trays was weighed (Day 0). Food weight was measured again two days later (Day 2), ensuring that any large pieces of food that had fallen into the cage were included in the measurement. Food intake in kcal was determined as follows: [($Weight_{Day\ 0}$ – $Weight_{Day\ 2}$) x Food Energy Density], where standard chow has an energy density of 13.0 kJ and 45% HFD a density of 19.7 kJ.

EchoMRI Analysis

Fat mass and lean mass were measured by the University of Ottawa Animal Behaviour Core (Ottawa, ON) at week 10 of the metabolic challenge using an EchoMRI-700 (EchoMRI LLC, Houston, TX, USA). Percent fat and lean mass were determined relative to total body weight measured immediately prior to doing the MRI. The instrument was calibrated as per the manufacturer's instructions prior to measurements.

Quantitative Real Time PCR

RNA was isolated from whole pancreas, liver, perirenal fat, placenta, and hypothalamic brain using TRIzol™ (#15596018, Invitrogen, Carlsbad, CA, USA) as per the manufacturer's instructions. DNase treatment was performed prior to cDNA synthesis with the iScript™ gDNA Clear cDNA Synthesis Kit (#1725035, Biorad, Mississauga, ON, Canada). qPCR was performed using SsoAdvanced Universal SYBR Green Supermix (Biorad, #1725271) or SensiFAST™ SYBR® No-ROX Supermix (# BIO-980050, Bioline, London, UK) and run on a CFX96 or CFX394 (Biorad). *Hprt*, *Ppia*, or *CypA* was used as the reference gene since these genes displayed stable expression under control and treatment conditions. Data were analyzed using the $2^{\Delta\Delta CT}$ relative quantitation method. Primer sequences are listed in **Table S1.**

Immunofluorescent Staining and Image Quantification

Whole pancreas tissues were processed and paraffin-embedded by the University of Ottawa Heart Institute Histology Core Facility (Ottawa, ON). Tissues were sectioned (5 µm thick) using a Thermo Scientific Microm HM 355S. Immunofluorescent staining was performed as previously described [8]. In brief, slides were deparaffinized with sequential incubations in xylene and ethanol. Heat-induced epitope retrieval was performed in 10 mM citrate buffer or 10 mM Tris base at 95°C for 10-15 minutes, and slides were incubated with Dako Serum Free Protein Block (#X090930-2, Agilent, Santa Clara, CA) for 30 minutes. Slides were incubated overnight at 4°C with primary antibodies, and then incubated with secondary antibodies for 1-hour at room temperature. Coverslips were mounted with Vectashield® hardset mounting medium with DAPI (#H-1500, Vector Laboratories, Burlingame, CA, USA) or ProLong Gold antifade mountant (Thermo Fisher Scientific, #P36935) for counterstaining nuclei.

The following primary antibodies were used: rabbit anti-insulin (1:200, C27C9, Cell Signaling Technology, Danvers, MA, USA; #3014), mouse anti-insulin (1:250, L6B10, Cell Signaling, #8138S), mouse anti-glucagon (1:250, Sigma-Aldrich, #G2654), mouse anti-PCNA (1:100, BD Transduction Laboratories, San Jose, CA, USA; #610665), rabbit anti-MAFA (1:1000, shared by Dr. Timothy Kieffer), and mouse anti-proinsulin (1:50, DSHB, Iowa City, IA, USA; GS-9A8-s). The following secondary antibodies were used: goat anti-rabbit IgG (H+L) secondary antibody, Alexa Fluor 594 (1:1000, Invitrogen, #A11037); and goat anti-mouse IgG (H+L) secondary antibody, Alexa Fluor 488 (1:1000, Invitrogen, #A11029).

For islet morphology quantification, a minimum of five islets were imaged and analysed with an Axio Observer 7 microscope Zen Blue 2.6 software (Carl Zeiss, Germany), and the average value was calculated for each mouse. The % hormone$^+$ area per islet was calculated as [(hormone$^+$ area / islet area) x 100]. The % PCNA$^+$ insulin$^+$ cells per islet was calculated as [(# of PCNA$^+$ insulin$^+$ cells) / (total # of insulin$^+$ cells per islet) x 100]. The % MAFA$^-$ insulin$^+$ cells per islet was calculated as [(# of MAFA$^-$ insulin$^+$ cells per islet) / (total # of insulin$^+$ cells per islet) x 100]. The % beta cells with accumulation proinsulin was calculated as [(# of insulin$^+$ cells with accumulated cytoplasmic proinsulin) / (total # of insulin$^+$ cells per islet) x 100].

Quantification and Statistical Analysis

All statistics were performed using GraphPad Prism 8.4.2 (GraphPad Software Inc., La Jolla, CA). Specific statistical tests are indicated in Fig. legends and in **Table S2**. Verification of parametric assumptions are found in **Table S2**. Sample sizes are described in ***Animals*** and are also shown in the schematic timeline (**Fig. 1A**). For all analyses, $p<0.05$ was considered statistically significant. Statistically significant outliers were detected by a Grubbs' test with $\alpha=0.05$. All data was tested for normality using a Shapiro-Wilk test and for equal variance using either a Brown-Forsyth test (for one-way ANOVAs) or an F test (for unpaired t tests). Non-parametric statistics were used in cases where the data failed normality or equal variance tests. Parametric tests were used for all two-way ANOVAs, but normality and equal variance were tested on area under the curve values and by one-way ANOVAs (**Table S2**). A two-way mixed-effect model (REML) ANOVA was used in cases where data points were missing due to random reasons. Data are presented as mean ± SEM. Box and whisker plots display the mean with whiskers representing minimum to maximum values. Individual data points on box and whiskers plots are always biological replicates (i.e. different mice).

Data and Resource Availability
The datasets generated and/or analyzed during the current study are available from the corresponding author upon reasonable request. No applicable resources were generated or analyzed during the current study.

Results

Chronic low-dose TCDD exposure induces Cyp1a1 gene expression more strongly in the pancreas than other tissues at mid-gestation
Briefly, female mice were injected with either corn oil (CO; vehicle control) or 20 ng/kg/d TCDD 2x/week during mating, pregnancy, and lactation ("TCDD Injections" window), and then tracked for 6-10 weeks after chemical exposure stopped ("Post-TCDD" window) (**Fig. 1A**). A subset of CO- and TCDD-exposed dams were then transferred to a 45% HFD or remained on standard chow diet for an additional 11 weeks to assess long-term effects of TCDD on adaptability to a metabolic stressor ("Metabolic Challenge" window) (**Fig. 1A**).

Before examining the effects of chronic low-dose TCDD exposure on glucose homeostasis and beta cell adaptation during pregnancy, we first validated our model by ensuring that TCDD was reaching the dam pancreas mid-gestation using *Cyp1a1* as an indicator of direct pollutant exposure [8]. TCDD induced *Cyp1a1* expression ~17-fold in the pancreas compared to ~3-fold, ~8-fold, and ~3.5-fold increase in the liver, perirenal fat, and placenta, respectively at day 15.5 of pregnancy relative to control (**Fig. 1B**). *Ahr* expression was reduced ~2-fold in the pancreas and perirenal fat of TCDD-exposed dams compared to controls, and not changed in liver or placenta (**Fig. 1C**). *Arnt* was also reduced ~2-fold in the pancreas but was not changed in other tissues compared to control (**Fig. 1D**). These results indicate that TCDD reaches the pancreas of pregnant dams and strongly induces *Cyp1a1* expression, which leads to negative feedback regulation of the AhR pathway.

We also assessed whether TCDD exposure during pregnancy induced inflammatory stress in the dams or altered islet morphology. There were no changes in *Tnfα*, *Nf-κβ*, or *Il-1β* gene expression in the pancreas, liver, or placenta of TCDD-exposed dams at mid-gestation relative to control (**Fig. 1E-G**), except for a modest ~1.4-fold decrease in *Nf-κβ* levels in the placenta (**Fig. 1F**). Furthermore, islet morphology and beta cell characteristics mid-pregnancy were not affected by TCDD exposure, including average islet area (**Fig. 1H, 1M**), % insulin$^+$ area per islet (**Fig. 1I**), % glucagon$^+$ area per islet (**Fig. 1J**), % MAFA$^-$ beta cells (**Fig. 1K**), and % PCNA$^+$ beta cells (**Fig. 1L-M**). Therefore, chronic low-dose TCDD exposure during pregnancy does not influence beta cell proliferation, beta cell maturity, or islet composition at gestation day 15.5.

TCDD exposure during pregnancy and lactation promotes weight gain post-exposure
We next investigated whether transient TCDD exposure during pregnancy and lactation had short- or long-term effects on dam metabolism. TCDD-exposed dams were transiently hypoglycemic at postnatal day 1 (P1) compared to control dams (**Fig. 2A-inset**), but otherwise had normal fasting glycemia during TCDD exposure and for 10 weeks after exposure ended (i.e. post-TCDD; **Fig. 2A**). Importantly, the TCDD-induced hypoglycemia at P1 was replicated in a second independent cohort of mice (**Fig. S1A**). There were also no changes in fasting plasma insulin levels during pregnancy or lactation with either cohort (**Fig. 2C, S1C**) or in islet morphology of dam pancreas

at P1 (**Fig. S2A-G)**. Since we did not observe any signs of GDM development in TCDD-exposed dams, we did not perform glucose or insulin tolerance tests during pregnancy to avoid unnecessary stress. However, we did conduct extensive metabolic testing on the dams for 10 weeks after TCDD exposure stopped at the end of lactation. TCDD exposure did not cause any long-term changes to glucose tolerance (**Fig. 2D, 2G, S3B**), glucose-stimulated insulin secretion (**Fig. 2E, 2H, S3C**), or insulin tolerance (**Fig. 2F**) in the 10 weeks post-TCDD (i.e. week 7-17 of the study).

We also assessed the impact of TCDD on body weight during and post exposure. Throughout pregnancy TCDD-exposed dams had normal body weight (**Fig. 2B, S1B**) and food intake (**Fig. S3A**). However, TCDD-exposed dams were transiently heavier mid-lactation compared to controls (**Fig. 2B**), with no change in food intake (**Fig. S3A**). We also observed a modest but statistically significant increase in body weight in TCDD-exposed dams starting 5 weeks after their last TCDD exposure (**Fig. 2B**). Based on these results, we speculated that female mice who were exposed to TCDD during pregnancy and lactation might be more susceptible to weight gain when challenged with an obesogenic diet (45% HFD).

Transient TCDD exposure during pregnancy and lactation promotes diet-induced obesity and alters energy homeostasis in dams

Between 6-10 weeks after the last TCDD exposure (week 13-17 of the study), a subset of CO- and TCDD-exposed mice were transitioned to a 45% HFD (COHFD, TCDDHFD) while the other subset remained on standard chow (COChow, TCDDChow) for 11 weeks (see **Fig. 1A** for study timeline). Consistent with our findings in **Fig. 2A**, TCDDChow dams continued to maintain normal fasting glycemia compared to COChow dams throughout the study (**Fig. 3A**). HFD-fed dams developed moderate fasting hyperglycemia, irrespective of chemical exposure (**Fig. 3A**). During this "metabolic challenge" window, we were particularly interested in whether TCDD-induced weight gain would persist long-term (i.e. TCDDChow versus COChow), and whether HFD feeding would exacerbate these effects (i.e. TCDDHFD versus TCDDChow). The increased body weight in TCDDChow dams (**Fig. 2B**) returned to control levels after longer tracking (**Fig. 3B**). Interestingly, TCDDHFD dams showed a rapid and sustained increase in body weight starting 1 week after being transferred to a HFD, whereas COHFD dams only had a modest increase in body weight after ~10 weeks of HFD feeding (**Fig. 3B**). Both HFD-fed groups had significantly increased % fat mass and decreased % lean mass compared to chow-fed dams after 10 weeks of HFD feeding, but these changes in body composition were exacerbated in TCDDHFD dams compared to COHFD dams (**Fig. 3C**).

To better understand why TCDD-exposed mice gained more fat mass than control mice after HFD feeding, we investigated other changes in energy homeostasis. We observed a significant decrease in caloric intake in TCDDHFD dams after 7 weeks of HFD feeding compared to TCDDChow dams but this was not different than COHFD dams, so unlikely to explain the dramatic differences in weight gain between HFD groups (**Fig. 3D**). As expected, circulating leptin levels were significantly increased by ~7.7-fold in COHFD dams compared to COChow dams after 11 weeks on HFD (**Fig. 3E)**. In contrast, TCDDHFD dams only showed a non-significant trend towards having ~3-fold higher circulating leptin compared to TCDDChow dams, and leptin levels in TCDDHFD dams were significantly lower than COHFD dams (**Fig. 3E**). In order to assess the contribution of central energy balance in TCDD-mediated obesity, we measured gene expression of key regulators within the brain. Proopiomelanocotin (*Pomc*) expression in the hypothalamus

was also dramatically induced by HFD feeding in both CO- and TCDD-exposed dams, but levels were significantly lower in TCDDHFD dams compared to COHFD dams (**Fig. 3F**). There was no effect of diet or chemical exposure on gene expression of the agouti-related peptide (*Agrp*), leptin receptor (*Lepr*), or insulin receptor (*Insr*) in the hypothalamus after 11 weeks of HFD feeding (**Fig. 3F**). We did observe a significant decrease in neuropeptide Y (*Npy*) gene expression in TCDDChow dams compared to COChow dams, but no effect in TCDDHFD dams (**Fig. 3F**). Taken together, these data suggest that diet-induced weight gain in TCDD-exposed dams (relative to CO) may involve insufficient leptin levels, and consequently insufficient *Pomc* levels, thus promoting fat storage.

HFD feeding causes severe hyperglycemia in TCDD-exposed dams without altering insulin tolerance

Obesity is a major risk factor for developing diabetes, so even though there were no long-term changes in fasting glycemia as a result of TCDD exposure (**Fig. 3A**), we investigated whether the diet-induced weight gain seen in TCDDHFD dams was associated with changes in glucose or insulin tolerance. As expected, COHFD dams displayed modest hyperglycemia during a glucose tolerance test (GTT) after 2.5 weeks of HFD feeding (**Fig. 4A**). In contrast, TCDDHFD dams were severely hyperglycemic throughout the GTT, with a peak glycemia of ~30 mM compared to ~22 mM in COHFD dams (**Fig. 4A**), and a significant increase in overall glucose excursion compared to COHFD dams (**Fig. 4A-AUC**). Following 6.5 (**Fig. S4A**) and 9.5 weeks (**Fig. 4C**) of HFD feeding, both COHFD and TCDDHFD dams had similar levels of hyperglycemia during a GTT. There were no differences in overall insulin tolerance between any groups at weeks 4, 7, or 10.5 of the metabolic challenge (**Fig. 4B, 4D, S4B**).

HFD feeding impairs insulin secretion in TCDD-exposed dams

Since defective glycemic control may be triggered by improper insulin secretion, we assessed changes in glucose-stimulated insulin secretion (GSIS) following HFD feeding. Corresponding with the profound hyperglycemia observed after 2.5 weeks of HFD feeding (**Fig. 4A**), TCDDHFD dams had significantly lower plasma insulin levels 15 minutes following an intraperitoneal (i.p.) glucose bolus compared to COHFD dams (**Fig. 5Aiii**), and trended towards having reduced overall insulin secretion during the GTT compared to TCDDChow dams (**Fig. 5Aiv**). Interestingly, after 6.5 weeks of HFD feeding, TCDDHFD dams had significantly higher basal insulin levels compared to COHFD dams (**Fig. 5Biii**) and trended towards secreting more insulin overall during the GTT compared to TCDDChow dams (**Fig. 5Biv**). After 9.5 weeks of HFD feeding, insulin levels in TCDDHFD dams had normalized back to COHFD levels (**Fig. 5C iii,iv**). Prior TCDD exposure had no impact on insulin secretion in chow-fed dams (i.e. TCDDChow vs COChow) at any time point (**Fig. 5Aii-5Cii**).

HFD feeding following maternal TCDD exposure increases accumulation of proinsulin

Obesity-induced diabetes is partly mediated by chronic inflammation, oxidative stress, and ER stress leading to defects in insulin signalling and/or secretion [35]. As such, we next measured changes in inflammatory and stress markers in whole pancreas at week 11 of the metabolic challenge. Chemical exposure significantly reduced expression of inflammatory markers *Nf-κβ* and *Il-1β*, and oxidative stress markers *Nox2* and *Sod2*, while increasing the oxidative stress marker *Cat* (**Fig. 6A)**. These results suggest that TCDD alone may be associated with an attenuated inflammatory response, and some degree of oxidative stress. However, these modest changes are

unlikely to explain the diabetic phenotype observed in TCDDHFD dams. Interestingly, we observed an interactive effect of chemical exposure and diet on expression of the hypoxia marker *Hmox1* leading to a significant downregulation of *Hmox1* in TCDDHFD dams compared to COHFD dams (**Fig. 6B**). We also observed an interactive effect on expression of the ER stress marker *Bip*, however this is not likely to contribute to the phenotype seen in TCDDHFD dams since *Bip* expression was reduced in all groups compared to control (**Fig. 6B**). There were no changes in gene expression of the inflammatory marker *Tnf-α*, oxidative stress markers *Sod1*, *Cat*, *Gsr*, and *Gxp2*, ER stress markers *Chop*, *Ero1α*, and *Gadd34*, and the mitochondrial stress marker *UCP2* (**Fig. 6C**). Together these results suggest that TCDD alone may modestly suppress inflammatory responses in whole pancreas, and when combined with HFD may trigger a hypoxic state by suppressing *Hmox-1*.

Next, we assessed whether the observed changes in insulin secretion were associated with defects in endocrine hormone biosynthesis and/or processing by prohormone convertase enzymes PC1 and PC2. We observed a diet-induced decrease in both *Ins1* and *Ins2* gene expression in whole pancreas at week 11 of the metabolic challenge, and an interactive effect of chemical and diet on *Gcg* expression, which led to a significant or trending decrease in *Gcg* levels in all groups compared to COChow controls (**Fig. 6D**). Interestingly, diet and chemical exposure both altered *Pcsk1* expression, resulting in significantly decreased *Pcsk1* levels in TCDDHFD dams compared to COChow dams (**Fig. 6D**). In contrast, *Psck2* was downregulated in response to diet only (**Fig. 6D**). These data suggest that PC1 expression may be altered in TCDDHFD dams, which could lead to changes in proinsulin processing. Since gene expression was measured in whole pancreas, we next assessed plasma proinsulin levels and islet-specific proinsulin immunoreactivity. There was no change in the circulating proinsulin:insulin ratio in cardiac blood from random-fed mice at week 11 of the metabolic challenge (**Fig. 6E**). However, we did observe a significant increase in the proportion of beta cells with proinsulin accumulation throughout the cytoplasm as opposed to the expected perinuclear pattern of immunoreactivity in islets from TCDDHFD mice compared to TCDDChow and COHFD dams **(Fig. 6F-G**). These results suggest that the decrease in whole pancreas *Pcsk1* levels may reflect a defect in proinsulin processing at the islet level.

TCDDHFD dams have decreased islet size and a higher proportion of MAFA$^-$ beta cells compared to COHFD dams

Lastly, we assessed islet morphology and other beta cell characteristics at week 11 of the metabolic challenge. As expected, HFD feeding caused a significant ~2-fold increase in average islet size in control mice **(Fig. 7A, 7F, 7G**). However, TCDDHFD dams did not show the same adaptation to HFD feeding, but rather showed an average islet size that was comparable to chow-fed dams **(Fig. 7A, 7F, 7G**). We also observed that TCDDHFD dams had a significantly higher proportion of MAFA$^-$ beta cells compared to all other groups (**Fig. 7D, 7G**). There was no change in % insulin$^+$ area per islet (**Fig. 7B, 7F**), % glucagon$^+$ area per islet (**Fig. 7C, 7F**), or % PCNA$^+$ beta cells (**Fig. 7E**) in TCDDHFD dams compared to other groups. TCDDChow mice did not display any changes in islet composition compared to COChow dams (**Fig. 7A-G**).

Discussion

Our study demonstrates that low-dose exposure to TCDD throughout pregnancy and lactation has modest metabolic consequences during pregnancy but profoundly increases the susceptibility to weight gain and diabetes later in life. TCDD-exposed dams had normal body weight, basal blood glucose levels, plasma insulin levels, and beta cell plasticity during pregnancy, but were transiently hypoglycemic at birth and transiently heavier at 2 weeks post-birth compared to CO-exposed dams. After chemical exposure stopped at the end of lactation, TCDD-exposed dams maintained normal glucose homeostasis, but showed a modest increase in body weight compared to CO-exposed dams within 5 weeks post-TCDD. Once challenged with HFD feeding, TCDD-exposed dams rapidly became obese, severely glucose intolerant, and showed beta cell dysfunction. The TCDD-induced exacerbation of glucose intolerance and dysregulation of insulin secretion eventually resolved, but TCDDHFD mice remained significantly heavier than COHFD mice throughout the study. TCDD-exposed dams fed a HFD also displayed defects in insulin processing, reduced islet size, and a larger proportion of $MAFA^-$ beta cells compared to COHFD dams. Taken together, these data suggest that low-dose dioxin exposure during pregnancy and lactation leads to sustained susceptibility to developing obesity and diabetes long after exposure ceases.

To our knowledge, this is the first study assessing the association between chronic low-dose dioxin exposure during pregnancy/lactation and GDM or long-term diabetes risk in a mouse model. Our study shows that dioxins reach the pancreas and induce *Cyp1a1* expression during pregnancy. However, unlike previous studies in non-pregnant mice [8, 18], the degree of *Cyp1a1* induction in the pancreas was much higher than in the liver mid-pregnancy. It is unclear whether pregnancy promotes greater dioxin accumulation in the pancreas compared to other tissues or if the pancreas may be more sensitive to AhR-mediated dioxin signaling mid-pregnancy. Either way, we predicted that direct exposure of pancreatic tissue to dioxin during pregnancy could have immediate and long-term implications on islet physiology and diabetes risk. However, low-dose TCDD exposure alone did not cause overt GDM in this study. In fact, rather than developing hyperglycemia, we found that TCDD-exposed dams are transiently hypoglycemic at birth. Labour is an acute form of metabolic stress characterized by elevated blood glucose levels to compensate for increases in energy demand [36]. TCDD-induced hypoglycemia at birth suggests that dioxin exposure during pregnancy may impair the ability to adapt to a metabolic stressor; however, in the absence of a prolonged stressor the dams return to euglycemia. It would be of interest to determine in future studies whether combining TCDD exposure during pregnancy with a metabolic stressor, such as HFD feeding, would trigger the development of GDM.

Thus far, epidemiological studies investigating the association between POP exposure during pregnancy and diabetes incidence have been inconsistent. Some studies have shown a positive association between GDM and serum POP levels, including polychlorinated biphenyls (PCB) [29–31], polyfluoroalkyl (PFAS) [30], and polybrominated diphenyl ethers (PBDEs) [30, 32]. A positive association between GDM and self-reported pesticide exposure during pregnancy has also been reported [37]. However, other studies showed no association between GDM incidence and serum organochloride pesticides [32, 33] or PCB levels [33, 34]. Inconsistencies between human studies can result from the inability to control certain confounding variables, such as varying POP concentrations between participants, differences in timing of POP measurements, method of diabetes diagnosis, and genetics and environmental factors. Using a controlled mouse model, we demonstrated that chronic low-dose TCDD exposure did not impair body weight, basal blood glucose, plasma insulin levels, or beta cell plasticity acutely during pregnancy, but rather caused

long-term metabolic dysregulation. Therefore, epidemiological studies should consider tracking the metabolic health of mothers long-term following pollutant exposure during pregnancy.

The most persistent consequence of transient low-dose TCDD exposure during pregnancy and lactation was excessive weight gain later in life. TCDD-exposed dams showed modest weight gain in the absence of a metabolic stressor, but rapidly developed pronounced obesity following a transition to HFD feeding. These results are interesting given that acute high-dose TCDD exposure is known to cause wasting syndrome [8, 38]. To our knowledge this is the first study to report an increase in weight gain following chronic low-dose TCDD exposure. Whether low-dose TCDD exposure also promotes weight gain in non-pregnant mice remains to be investigated. Obesity in TCDDHFD dams was also associated with abnormal energy homeostasis. TCDDHFD dams had significantly reduced circulating leptin levels and hypothalamic *Pomc* levels compared to COHFD dams. Leptin is essential for regulating energy homeostasis and can activate POMC neurons in the hypothalamus [39, 40]. *Pomc* expression, especially in LepR POMC neurons, are critical for maintaining normal energy balance by providing anorexigenic drive [41]. Both leptin [42] and melanocortins produced by POMC neurons [43] can directly regulate peripheral lipid metabolism, and in effect leptin- and POMC-deficiency cause obesity by increasing food intake, limiting energy expenditure, and promoting fat storage [44–46]. We did not observe significant changes in food intake between TCDDHFD and COHFD dams but did find that TCDDHFD dams had significantly higher % fat mass than COHFD mice, suggesting an adaptation in energy expenditure and/or energy storage that promotes obesity. Studies using metabolic chambers would provide additional insight into the mechanisms underlying TCDD-induced weight gain in this model. Regardless, our data suggest that transient low-dose TCDD exposure during pregnancy may contribute to the rapid increase in obesity prevalence seen worldwide.

Being overweight is a well-established risk factor for developing type 2 diabetes. Indeed, transient TCDD exposure promoted diet-induced hyperglycemia which appears to be primarily driven by impaired beta cell plasticity and function. The rapid onset of hyperglycemia in TCDD-exposed mice after 2.5 weeks of HFD feeding coincided with suppressed glucose-induced insulin secretion, but no change in peripheral insulin sensitivity. Interestingly, the hypoinsulinemia in TCDDHFD dams transitioned to hyperinsulinemia, before eventually re-equilibrating back to COHFD levels, pointing to an initial defect in insulin secretion. TCDDHFD dams also had decreased islet size compared to COHFD dams, suggesting that TCDD-exposed beta cells lack the adaptive proliferative response to the metabolic demand of HFD feeding. However, without tissues from different timepoints, we cannot rule out the possibility that TCDDHFD mice experienced an appropriate increase in beta cell proliferation earlier, followed by an increase in beta cell apoptosis due to beta cell exhaustion. Decreased pancreatic expression of *Hmox1,* the gene that encodes heme-oxygenase 1, in TCDDHFD dams compared to COHFD dams could point to increased susceptibility to apoptosis, inflammation, and oxidative stress [47]. However, there were no significant changes in markers of inflammation or stress at this time point. It is important to note that these markers were measured in whole pancreas which may mask any effects occurring specifically in islets. At the islet level, we found that TCDDHFD dams had a modest but significant increase in $MAFA^-$ beta cells. MAFA is a transcription factor essential in maintaining beta cell maturity and function. Loss of MAFA causes beta cell dedifferentiation by suppressing genes critical for beta cell function, such as *Pcsk1* [48]; MAFA is also commonly supressed in beta cells from humans with type 2 diabetes [49, 50]. Interestingly, TCDDHFD dams also had reduced *Pcsk1*

expression in whole pancreas and an increased proportion of beta cells with cytoplasmic proinsulin accumulation, which is indicative of impaired insulin processing. Taken together, these results suggest that maternal TCDD exposure may induce beta cell dedifferentiation following HFD feeding, thereby increasing diabetes risk.

Epidemiological studies have consistently shown an association between exposure to dioxin/dioxin-like compounds and diabetes risk. However, limited studies have looked at the association between dioxin exposure during pregnancy and subsequent diabetes risk. Our study shows that chronic low-dose TCDD exposure during pregnancy was insufficient to induce GDM, but eventually led to impaired metabolic adaptability to HFD feeding, including glucose intolerance, beta cell dysfunction, and increased weight gain in mice. Therefore, background exposure to dioxin or dioxin-like chemicals may be contributing to the rapid rise in obesity and diabetes incidence seen worldwide. This emphasizes the need to further investigate the effects of low-dose pollutant exposure on metabolism.

Acknowledgements

This research was supported by a Canadian Institutes of Health Research (CIHR) Project Grant (#PJT-2018-159590), Natural Sciences and Engineering Research Council of Canada (NSERC) Discovery Grant (RGPIN-2017-06272), the Canadian Foundation for Innovation John R. Evans Leaders Fund (#37231), and an Ontario Research Fund award. M.P.H. was supported by an Ontario Graduate Scholarship (OGS) and CIHR CGS-D award. M.A.P. was supported by an OGS and Queen Elizabeth II Scholarship. H.B. received a NSERC Undergraduate Student Research Award (USRA) and a Carleton University Walker Summer Research Award. C.D.S. received a NSERC USRA and Carleton University I-CUREUS internship award. J.E.B. is the guarantor for this work.

Author Contributions

J.E.B. and M.P.H. conceived the experimental design and wrote the manuscript. M.P.H., R.C.M., H.B., C.D.S., M.A.P., D.I.M.A., M.Z., M.J.C., and J.E.B. were involved with acquisition, analysis, and interpretation of data. All authors contributed to manuscript revisions and approved the final version of the article.

Declaration of Interest

The authors declare no competing interests.

Figures

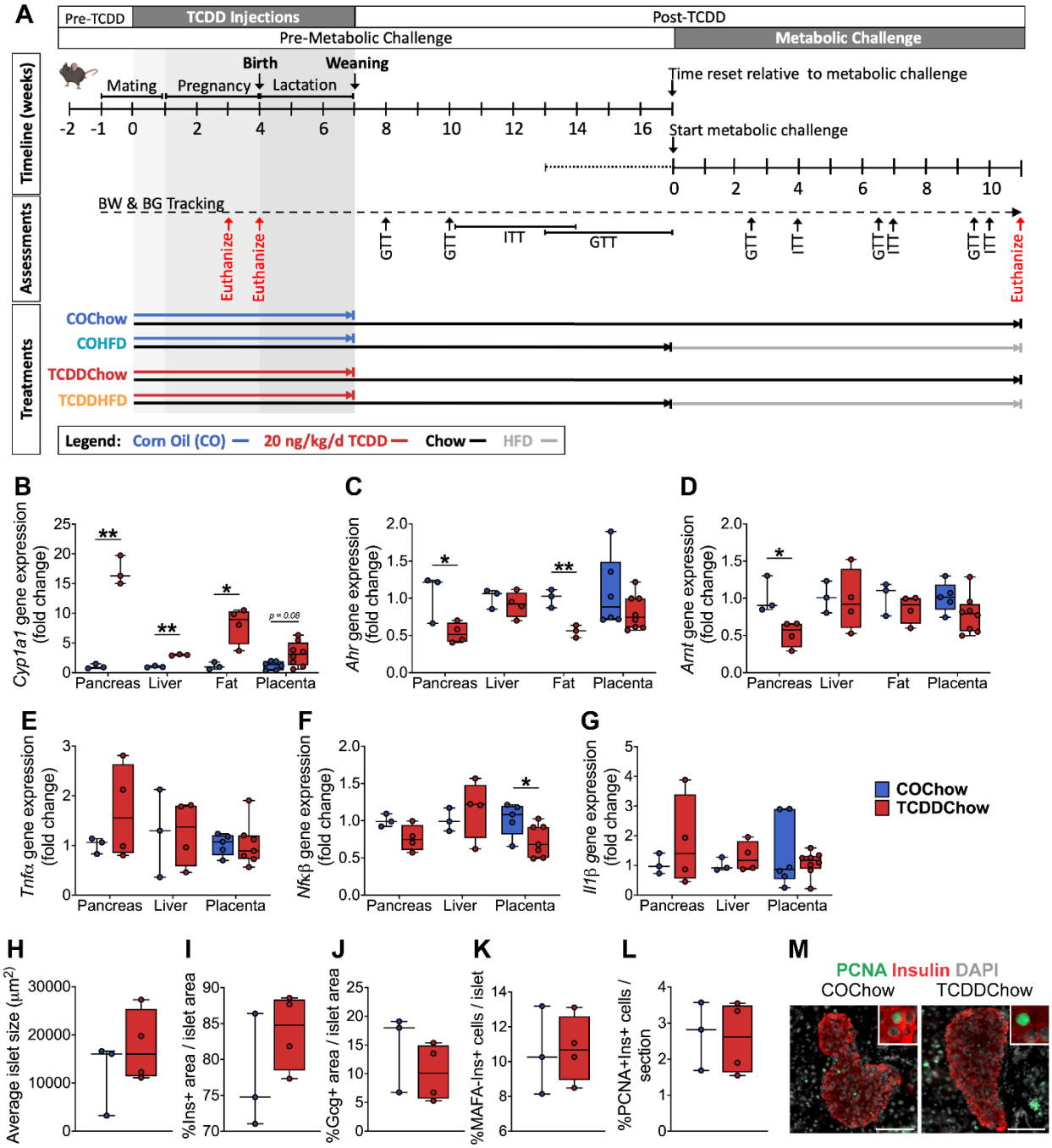

Fig. 1: Chronic low-dose TCDD exposure induces *Cyp1a1* expression more strongly in the pancreas than other tissues at mid-gestation. (**A**) Schematic summary timeline of the study. Female mice were injected with either corn oil (CO) or 20 ng/kg/d TCDD twice per week during mating, pregnancy, and lactation ("TCDD Injections" window), and then tracked for 6-10 weeks after chemical exposure stopped ("Post-TCDD" window) (i.e. week 13-17 of the study). This range reflects differences in the duration of mating, with a 4 week difference between the first and last pregnancies. At weeks 13-17 of the study, a subset of CO- and TCDD-exposed dams were

transitioned to a 45% HFD or remained on standard chow. All mice were then assessed for another 11 weeks. BW = body weight; BG = blood glucose; GTT = glucose tolerance test; ITT = insulin tolerance test. (**B-G**) Gene expression was measured in various tissues on day 15.5 of pregnancy. Gene levels are expressed as fold change relative to control. (**B**) *Cyp1a1*, (**C**) *Ahr*, and (**D**) *Arnt* gene expression were measured in whole pancreas, liver, perirenal fat, and placenta. (**E**) *Tnfα*, (**F**) *Nf-κβ*, and (**G**) *Il-1β* gene expression were measured in whole pancreas, liver, and placenta. (**H-M**) Histological analysis of pancreas collected from dams mid-gestation, including quantification of (**H**) average islet area, (**I**) % insulin$^+$ area / islet area, (**J**) % glucagon$^+$ area / islet area, (**K**) % MAFA$^-$INS$^+$ cells per islet, and (**L**) % PCNA$^+$INS$^+$ cells per pancreas section. (**M**) Representative images of pancreas sections showing immunofluorescent staining for insulin and PCNA. Inset regions show PCNA$^+$INS$^+$ cells. Scale bar = 100 μm. All data are presented as mean ± SEM. Individual data points on box and whisker plots represent biological replicates (different mice). *$p<0.05$, **$p<0.01$ versus control. The following statistical tests were used: (**B, G**) two-tailed unpaired t-test for pancreas, liver, and fat; Mann Whitney Test for placenta; (**C-F, H-L**) two-tailed unpaired t-test.

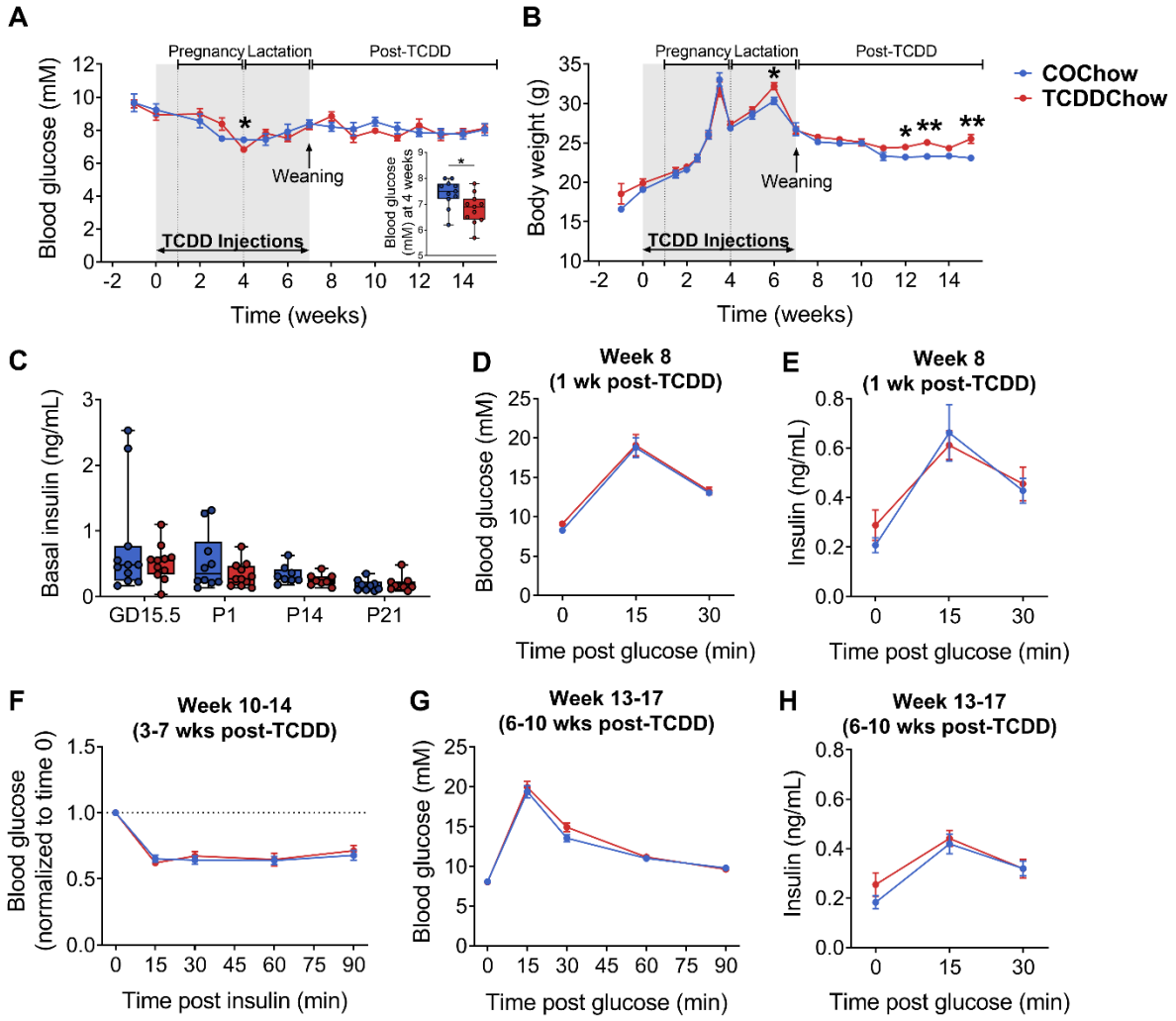

Fig. 2: Transient TCDD exposure during pregnancy and lactation causes hypoglycemia at birth and promotes weight gain post-exposure. Female mice were injected with either corn oil (CO) or 20 ng/kg/d TCDD 2x/week during mating, pregnancy, and lactation, and then tracked for 6-10 weeks after exposure (see **Fig. 1A** for study timeline). GTT = glucose tolerance test; ITT = insulin tolerance test. (**A**) Blood glucose and (**B**) body weight were measured weekly following a 4-hour morning fast. Blood glucose at postnatal day 1 (P1) is shown in the inset graph in (**A**). (**C**) Plasma insulin levels were measured at day 15.5 of pregnancy, P1, mid-lactation (P14), and weaning (P21) following a 4-hour morning fast. (**D, G**) Blood glucose and (**E, H**) plasma insulin levels during a GTT at (**D, E**) 1 week post-TCDD (i.e. week 8 of the study) and (**G, H**) 6-10 weeks post-TCDD (week 13-17 of the study). (**F**) Blood glucose levels during an ITT at 3-7 weeks post-TCDD (week 10-14 of the study) (values are normalized relative to time zero for each mouse). All data are presented as mean ± SEM. Individual data points on box and whisker plots represent biological replicates (different mice). *p <0.05, **p <0.01 versus control. The following statistical tests were used: (**A, B**) line graphs, two-way REML-ANOVA with uncorrected Fisher's LSD test; box and whisker plots, two-tailed unpaired t-test; (**C**) two-tailed unpaired t-test at P14; two-tailed Mann-Whitney test at GD15, P0, and P12; (**D-H**) two-way RM ANOVA with Sidak test.

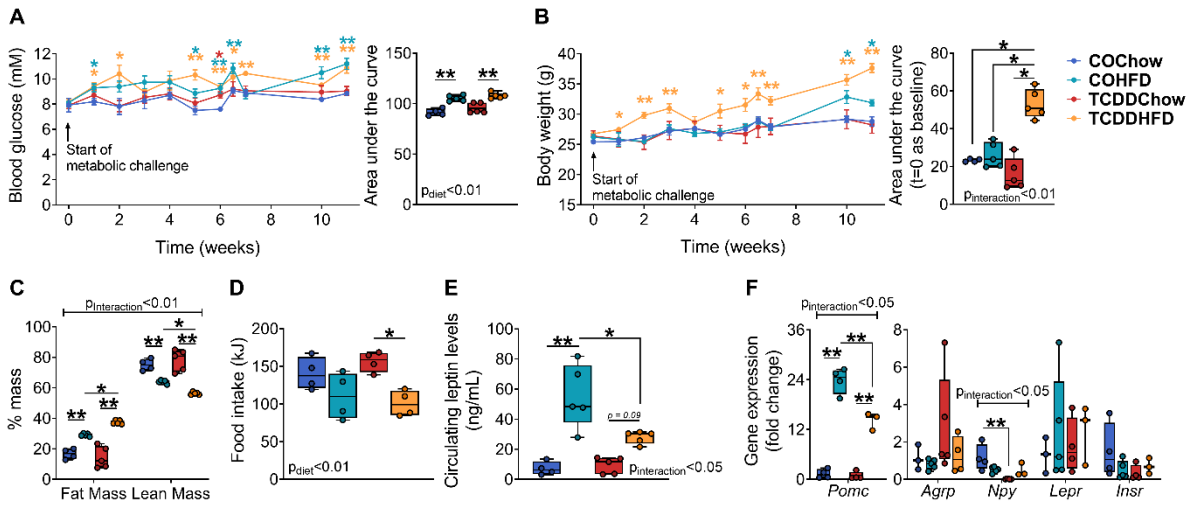

Fig. 3: TCDD exposure promotes diet-induced obesity in dams and alters energy homeostasis. Following 6-10 weeks of post-TCDD tracking in chow-fed mice (i.e. weeks 13-17 of the study), a subset of CO- and TCDD-exposed dams were transitioned to a 45% HFD or remained on standard chow and assessed for another 11 weeks ("Metabolic Challenge" window) (see **Fig. 1A** for study timeline). (**A**) Blood glucose and (**B**) body weight were measured weekly following a 4-hour morning fast. (**C**) % fat mass and lean mass were measured by EchoMRI 10 weeks into the metabolic challenge. (**D**) Caloric intake was measured at week 7 of the challenge. (**E**) Circulating leptin levels were measured in cardiac blood of random-fed dams at week 11 of the challenge. (**F**) Gene expression for markers of energy homeostasis were measured in the hypothalamus at week 11 of the challenge. All data are presented as mean ± SEM. Individual data points on box and whisker plots represent biological replicates (different mice). *p <0.05, **p<0.01, coloured stars are versus COChow. The following statistical tests were used: (**A, B**) line graphs, two-way RM ANOVA with uncorrected Fisher's LSD test; box and whisker plots, two-way ANOVA with Tukey's multiple comparison test; (**C-F**) two-way ANOVA with Tukey's multiple comparison test.

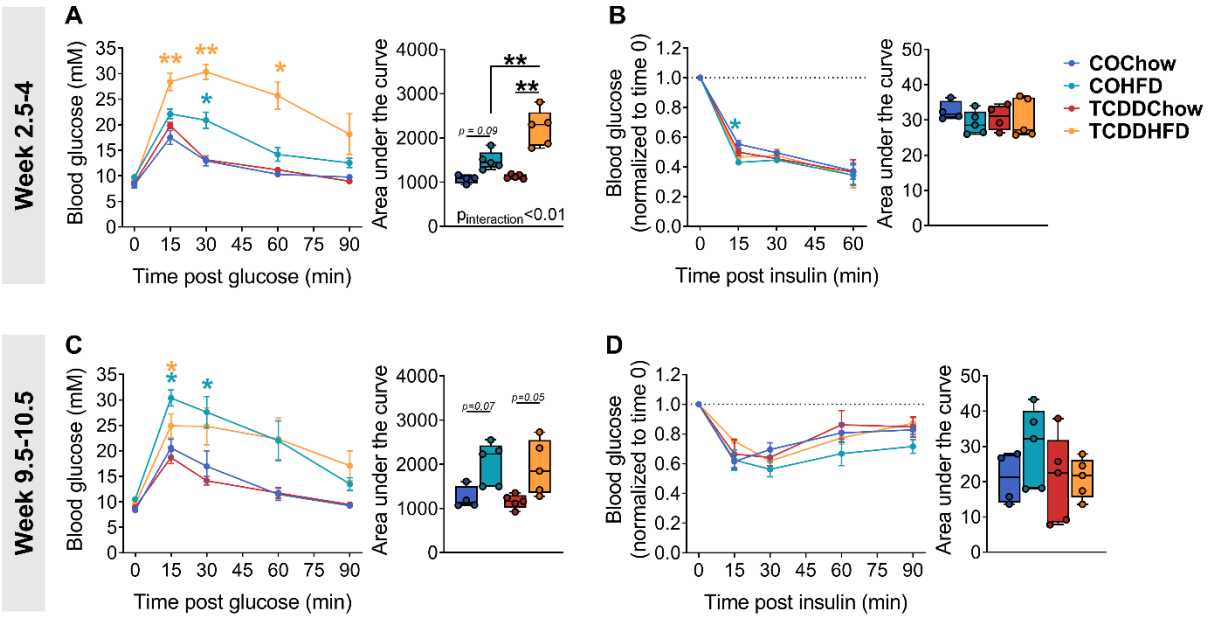

Fig. 4: HFD feeding causes severe hyperglycemia in TCDD-exposed dams without altering insulin tolerance. Glucose and insulin tolerance were assessed *in vivo* at weeks 2.5-4 and 9.5-10.5 of the metabolic challenge (see **Fig. 1A** for study timeline). (**A, C**) Blood glucose levels during a glucose-tolerance test at (**A**) week 2.5 and (**C**) week 9.5 of the metabolic challenge. (**B, D**) Blood glucose levels during an insulin tolerance test at (**B**) week 4 and (**D**) week 10.5 of the metabolic challenge (values are normalized relative to time zero for each mouse). All data are presented as mean ± SEM. Individual data points on box and whisker plots represent biological replicates (different mice). *p <0.05, **p <0.01, coloured stars are versus COChow. The following statistical tests were used: (**A-D**) line graphs, two-way RM ANOVA with Tukey's multiple comparison test; box and whisker plots, two-way ANOVA with Tukey's multiple comparison test.

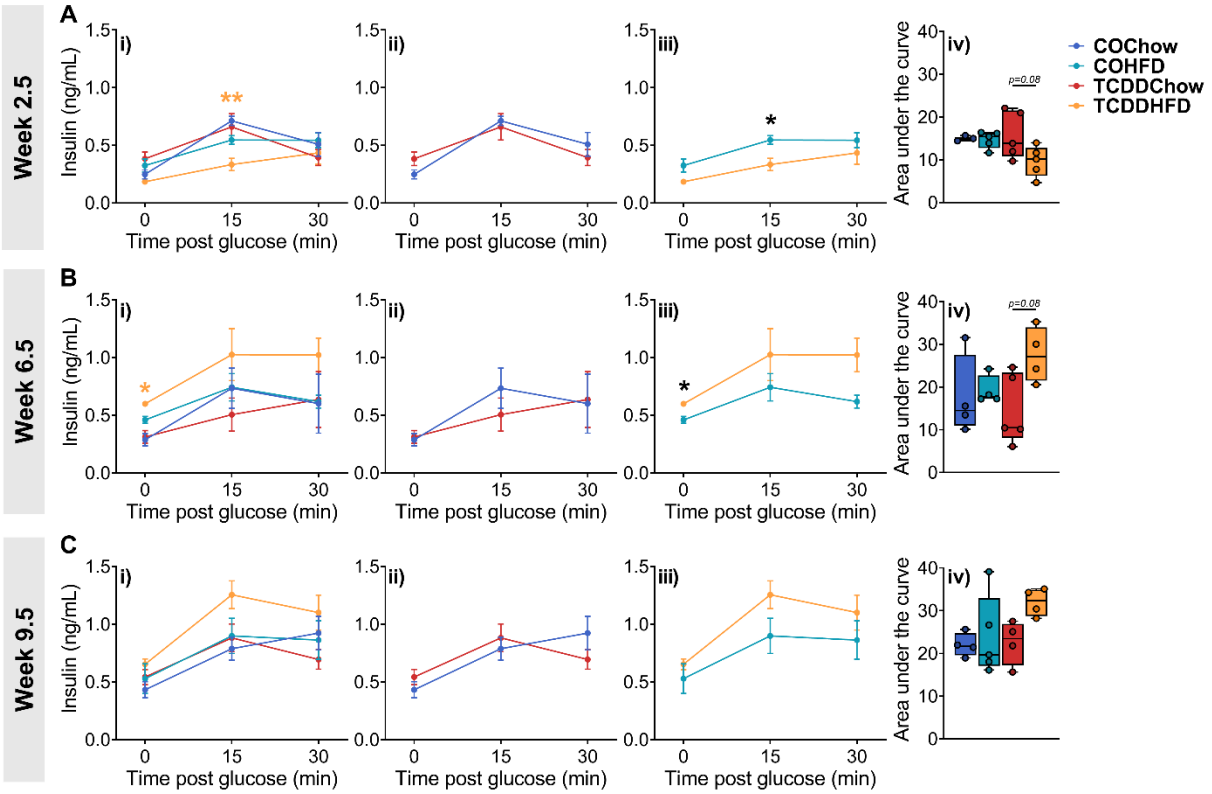

Fig. 5: HFD feeding impairs insulin secretion in TCDD-exposed dams. Glucose-stimulated insulin secretion was assessed *in vivo* at (**A**) week 2.5, (**B**) week 6.5, and (**C**) week 9.5 of the metabolic challenge (see **Fig. 1A** for study timeline). Insulin data are presented as (**i**) all groups compared to COChow, (**ii**) TCDDChow versus COChow, (**iii**) TCDDHFD compared to COHFD, and (**iv**) area under the curve for all groups. All data are presented as mean ± SEM. Individual data points on box and whisker plots represent biological replicates (different mice). *p <0.05, coloured stars are versus COChow. The following statistical tests were used: (**A-C i**) two-way RM ANOVA with Tukey's multiple comparison test; (**A-C ii**, **iii**) two-way RM ANOVA with Sidak test; (**A-C iv**) two-way ANOVA with Tukey's multiple comparison test.

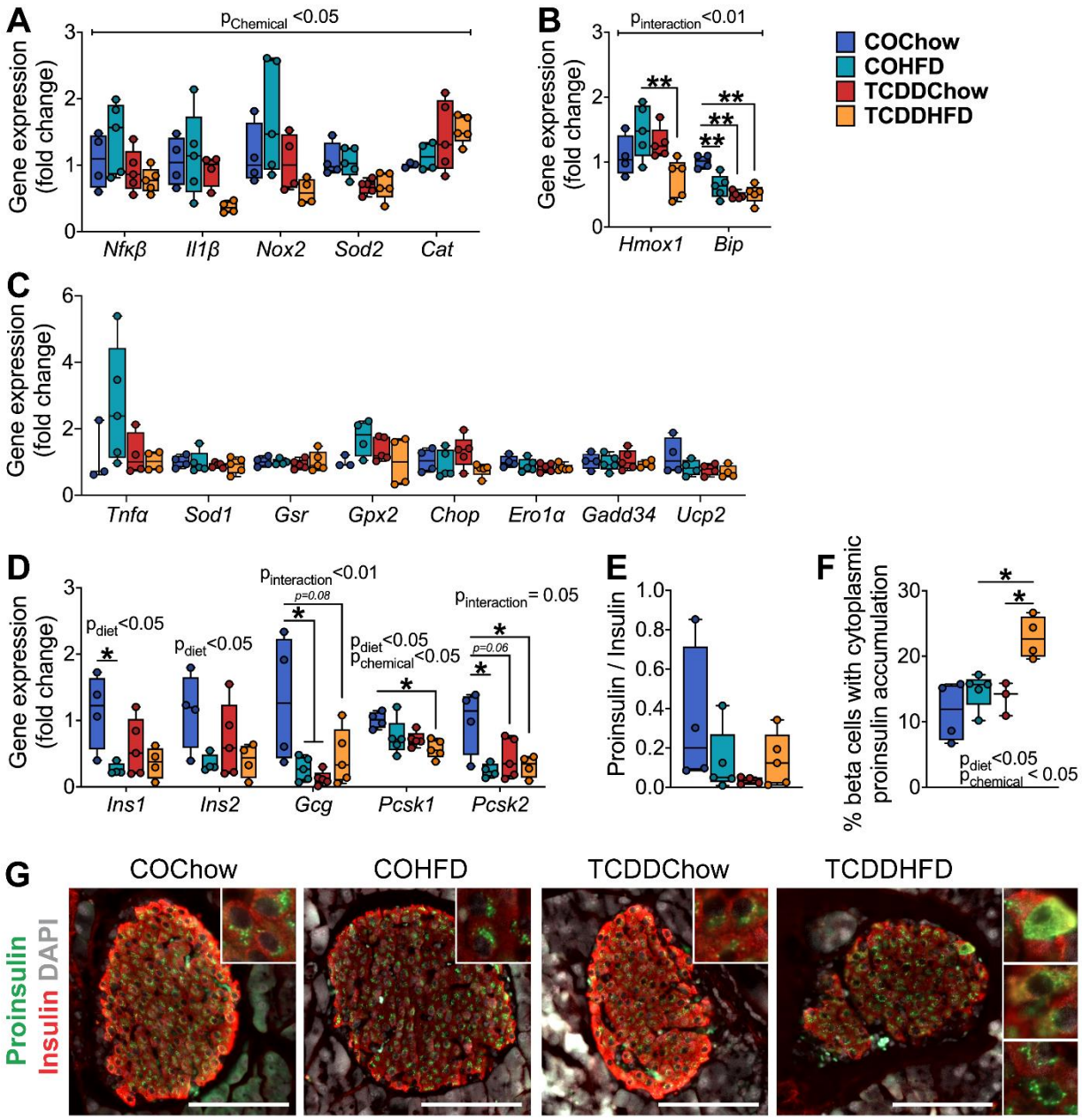

Fig. 6: HFD feeding following maternal TCDD exposure leads to impaired proinsulin processing. Whole pancreas and cardiac blood were harvested at week 11 of the metabolic challenge for analysis (see **Fig. 1A** for study timeline). (**A-C**) Gene expression of stress markers in the pancreas that (**A**) were significantly altered by chemical exposure, (**B**) showed a significant interaction between chemical exposure and diet, (**C**) were not significantly changed by chemical and/or diet exposure. (**D**) Gene expression of pancreatic hormones and hormone processing enzymes. (**E**) Circulating proinsulin/insulin levels in cardiac blood of random-fed dams. (**F**) % beta cells with cytoplasmic proinsulin accumulation, as determined by immunofluorescent staining. (**G**) Representative images of pancreas sections showing immunoreactivity for insulin and proinsulin. Inset regions show perinuclear proinsulin immunoreactivity versus proinsulin accumulation in the cytoplasm. Scale bar =100 µm. All data are presented as mean ± SEM.

Individual data points on box and whisker plots represent biological replicates (different mice). *p <0.05, **p <0.01. The following statistical tests were used: (**A-F**) two-way ANOVA with Tukey's multiple comparison test.

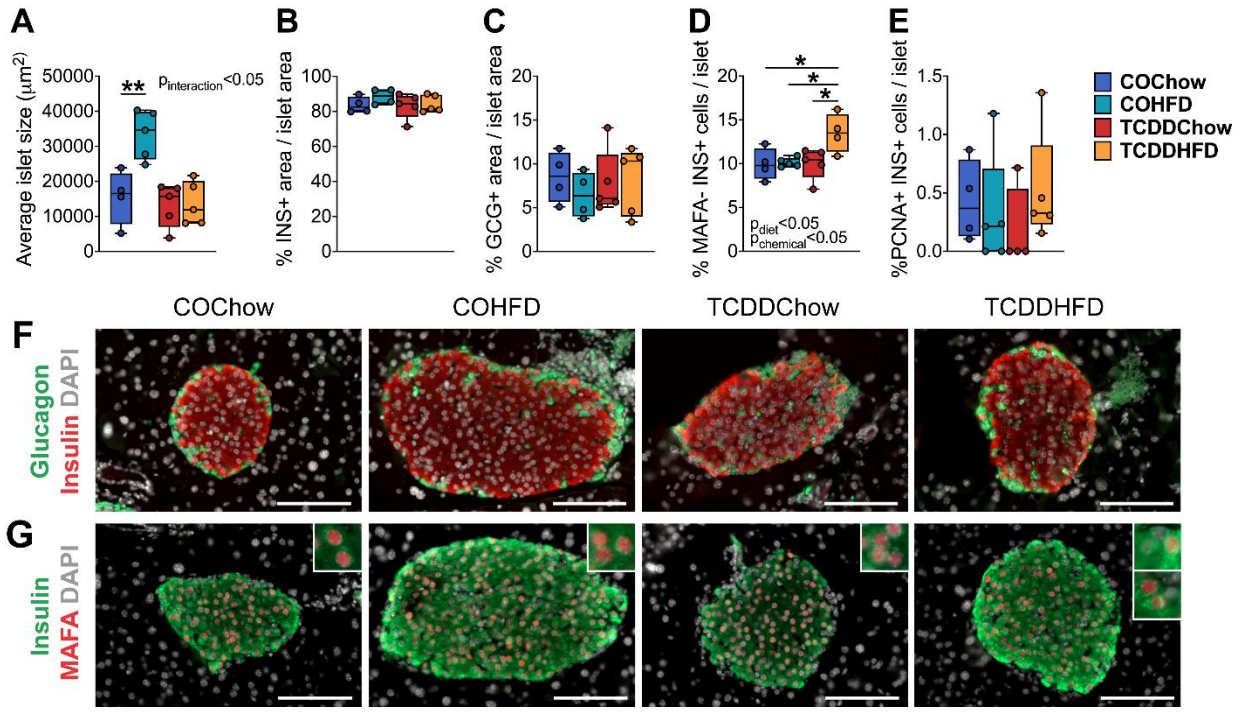

Fig. 7: TCDD-exposed dams fed a HFD have decreased islet size and a higher proportion of MAFA- beta cells. Whole pancreas was harvested at week 11 of the metabolic challenge for analysis by immunofluorescence staining (see **Fig. 1A** for study timeline). (**A**) Average islet area, (**B**) % islet$^+$ area / islet area, (**C**) % glucagon$^+$ area / islet area, (**D**) MAFA$^-$INS$^+$ cells per islet, and (**E**) % PCNA$^+$INS$^+$ cells per islet. (**F-G**) Representative images of pancreas sections showing immunofluorescence staining for (**F**) insulin/glucagon or (**G**) insulin/MAFA. Inset regions in **(G)** show MAFA$^+$INS$^+$ cells. Scale bar = 100 μm. All data are presented as mean ± SEM. Individual data points on box and whisker plots represent biological replicates (different mice). *p <0.05, **p <0.01. The following statistical tests were used: (**A-E**) two-way ANOVA with Tukey's multiple comparison test.

References

1. IDF (2019) IDF Diabetes Atlas, 9th Edition. https://www.diabetesatlas.org/en/

2. Wu Y, Ding Y, Tanaka Y, Zhang W (2014) Risk factors contributing to type 2 diabetes and recent advances in the treatment and prevention. Int J Med Sci 11(11):1185–1200. https://doi.org/10.7150/ijms.10001

3. Taylor KW, Novak RF, Anderson HA, et al (2013) Evaluation of the association between persistent organic pollutants (POPs) and diabetes in epidemiological studies: a national toxicology program workshop review. Environ Heal Perspect 121(7):774–783. https://doi.org/10.1289/ehp.1205502

4. Sun W, Clark JM, Park Y (2017) Environmental pollutants and type 2 diabetes: a review of human studies. Toxicol Environemtnal Chem 99(9–10):1283–1303. https://doi.org/https://doi.org/10.1080/02772248.2017.1393818

5. Breivik K, Alcock R, Li YF, Bailey RE, Fiedler H, Pacyna JM (2004) Primary sources of selected POPs: regional and global scale emission inventories. Environ Pollut 128(1–2):3–16. https://doi.org/10.1016/j.envpol.2003.08.031

6. White SS, Birnbaum LS (2009) An overview of the effects of dioxins and dioxin-like compounds on vertebrates, as documented in human and ecological epidemiology. J. Environ. Sci. Heal. - Part C Environ. Carcinog. Ecotoxicol. Rev.

7. Mimura J, Fujii-Kuriyama Y (2003) Functional role of AhR in the expression of toxic effects by TCDD. Biochim Biophys Acta - Gen Subj 1619(3):263–268. https://doi.org/10.1016/S0304-4165(02)00485-3

8. Ibrahim M, MacFarlane EM, Matteo G, et al (2020) Functional cytochrome P450 1a enzymes are induced in mouse and human islets following pollutant exposure. Diabetologia 63:162–178. https://doi.org/https://doi.org/10.1007/s00125-019-05035-0

9. Lee DH, Steffes MW, Sjödin A, Jones RS, Needham LL, Jacobs DR (2011) Low dose organochlorine pesticides and polychlorinated biphenyls predict obesity, dyslipidemia, and insulin resistance among people free of diabetes. PLoS One 6(1):e15977. https://doi.org/10.1371/journal.pone.0015977

10. Chang JW, Chen HL, Su HJ, Liao PC, Guo HR, Lee CC (2010) Dioxin exposure and insulin resistance in Taiwanese living near a highly contaminated area. Epidemiology 21:56–61. https://doi.org/10.1097/EDE.0b013e3181c2fc6e

11. Cranmer M (2000) Exposure to 2,3,7,8-tetrachlorodibenzo-p-dioxin (TCDD) is associated with hyperinsulinemia and insulin resistance. Toxicol Sci 56:431–436. https://doi.org/10.1093/toxsci/56.2.431

12. Pesatori AC, Zocchetti C, Guercilena S, Consonni D, Turrini D, Bertazzi PA (1998) Dioxin exposure and non-malignant health effects: a mortality study. Occup Environ Med 55:126–131. https://doi.org/10.1136/oem.55.2.126

13. Consonni D, Pesatori AC, Zocchetti C, et al (2008) Mortality in a population exposed to dioxin after the Seveso, Italy, accident in 1976: 25 years of follow-up. Am J Epidemiol

167(7):847–858. https://doi.org/10.1093/aje/kwm371

14. Vasiliu O, Cameron L, Gardiner J, DeGuire P, Karmaus W (2006) Polybrominated biphenyls, polychlorinated biphenyls, body weight, and incidence of adult-onset diabetes mellitus. Epidemiology 17:352–359. https://doi.org/10.1097/01.ede.0000220553.84350.c5

15. Wang SL, Tsai PC, Yang CY, Guo YL (2008) Increased risk of diabetes and polychlorinated biphenyls and dioxins: a 24-year follow-up study of the Yucheng cohort. Diabetes Care 31(8):1574–1579. https://doi.org/10.2337/dc07-2449

16. Rylander L, Rignell-Hydbom A, Hagmar L (2005) A cross-sectional study of the association between persistent organochlorine pollutants and diabetes. Environ Heal A Glob Access Sci Source 4:28. https://doi.org/10.1186/1476-069X-4-28

17. Airaksinen R, Rantakokko P, Eriksson JG, Blomstedt P, Kajantie E, Kiviranta H (2011) Association between type 2 diabetes and exposure to persistent organic pollutants. Diabetes Care 34(9):1972–2303. https://doi.org/10.2337/dc10-2303

18. Hoyeck MP, Blair H, Ibrahim M, et al (2020) Long-term metabolic consequences of acute dioxin exposure differ between male and female mice. Sci Rep 10(1):1448. https://doi.org/https://doi.org/10.1101/762476

19. Lee YM, Ha CM, Kim SA, et al (2017) Low-dose persistent organic pollutants impair insulin secretory function of pancreatic b-cells: human and in vitro evidence. Diabetes 66(10):2669–2680. https://doi.org/10.2337/db17-0188

20. Novelli M, Piaggi S, De Tata V (2005) 2,3,7,8-Tetrachlorodibenzo-p-dioxin-induced impairment of glucose-stimulated insulin secretion in isolated rat pancreatic islets. Toxicol Lett 156(2):307–314. https://doi.org/10.1016/j.toxlet.2004.12.004

21. Mailloux R, Fu A, Florian M, et al (2015) A Northern contaminant mixture impairs pancreas function in obese and lean JCR rats and inhibits insulin secretion in MIN6 cells. Toxicology 334:81–93. https://doi.org/10.1016/j.tox.2015.06.001

22. Steenland K, Piacitelli L, Deddens J, Fingerhut M, Chang LI (1999) Cancer, heart disease, and diabetes in workers exposed to 2,3,7,8- tetrachlorodibenzop-dioxin. J Natl Cancer Inst 91:779–786. https://doi.org/10.1093/jnci/91.9.779

23. Glynn AW, Granath F, Aune M, et al (2003) Organochlorines in Swedish women: determinants of serum concentrations. Environ Health Perspect 111:349–355. https://doi.org/10.1289/ehp.5456

24. Sorenson RL, Brelje TC (1997) Adaptation of islets of Langerhans to pregnancy: β-cell growth, enhanced insulin secretion and the role of lactogenic hormones. Horm Metab Res 29(6):301–307. https://doi.org/10.1055/s-2007-979040

25. Karnik SK, Chen H, McLean GW, et al (2007) Menin controls growth of pancreatic β-cells in pregnant mice and promotes gestational diabetes mellitus. Science (80-) 318:806–809. https://doi.org/10.1126/science.1146812

26. Van Assche FA, Aerts L, Prins F De (1978) A morphological study of the endocrine pancreas in human pregnancy. Br J Obstet Gynaecol 85:818–80.

https://doi.org/10.1111/j.1471-0528.1978.tb15835.x

27. Butler AE, Cao-Minh L, R. Galasso, et al (2010) Adaptive changes in pancreatic beta cell fractional area and beta cell turnover in human pregnancy. Diabetologia 53(10):2167–2176. https://doi.org/10.1007/s00125-010-1809-6

28. Moyce BL, Dolinsky VW (2018) Maternal β-Cell adaptations in pregnancy and placental signalling: implications for gestational diabetes. Int J Mol Sci 19(11):3467. https://doi.org/10.3390/ijms19113467

29. Longnecker MP, Klebanoff MA, Brock JW, Zhou H (2001) Polychlorinated biphenyl serum levels in pregnant subjects with diabetes. Diabetes Care 24:1099–1101. https://doi.org/10.2337/diacare.24.6.1099

30. Rahman ML, Zhang C, Smarr MM, et al (2019) Persistent organic pollutants and gestational diabetes: a multi-center prospective cohort study of healthy US women. Environ Int 124:249–258. https://doi.org/10.1016/j.envint.2019.01.027

31. Vafeiadi M, Roumeliotaki T, Chalkiadaki G, et al (2017) Persistent organic pollutants in early pregnancy and risk of gestational diabetes mellitus. Environ Int 98:89–95. https://doi.org/10.1016/j.envint.2016.10.005

32. Smarr MM, Grantz KL, Zhang C, et al (2016) Persistent organic pollutants and pregnancy complications. Sci Total Environ 151–152:285–291. https://doi.org/10.1016/j.scitotenv.2016.02.030

33. Shapiro GD, Dodds L, Arbuckle TE, et al (2016) Exposure to organophosphorus and organochlorine pesticides, perfluoroalkyl substances, and polychlorinated biphenyls in pregnancy and the association with impaired glucose tolerance and gestational diabetes mellitus: the MIREC Study. Environ Res 147:71–81. https://doi.org/10.1016/j.envres.2016.01.040

34. Jaacks LM, Barr DB, Sundaram R, Maisog JM, Zhang C, Buck Louis GM (2016) Pre-pregnancy maternal exposure to polybrominated and polychlorinated biphenyls and gestational diabetes: a prospective cohort study. Environ Heal A Glob Access Sci Source 15:11. https://doi.org/10.1186/s12940-016-0092-5

35. Khodabandehloo H, Gorgani-Firuzjaee S, Panahi G, Meshkani R (2016) Molecular and cellular mechanisms linking inflammation to insulin resistance and β-cell dysfunction. Transl Res 167:228–256. https://doi.org/10.1016/j.trsl.2015.08.011

36. Scheepers HCJ, De Jong PA, Essed GGM, Kanhai HHH (2001) Fetal and maternal energy metabolism during labor in relation to the available caloric substrate. J Perinat Med 29:457–464. https://doi.org/10.1515/JPM.2001.064

37. Saldana TM, Basso O, Hoppin JA, et al (2007) Pesticide exposure and self-reported gestational diabetes mellitus in the agricultural health study. Diabetes Care 30(3):529–534. https://doi.org/10.2337/dc06-1832

38. Uno S, Dalton TP, Sinclair PR, et al (2004) Cyp1a1(-/-) male mice: protection against high-dose TCDD-induced lethality and wasting syndrome, and resistance to intrahepatocyte lipid accumulation and uroporphyria. Toxicol Appl Pharmacol

196(3):410–421. https://doi.org/10.1016/j.taap.2004.01.014

39. Cowley MA, Smart JL, Rubinstein M, et al (2001) Leptin activates anorexigenic POMC neurons through a neural network in the arcuate nucleus. Nature 24(411):480–484. https://doi.org/10.1038/35078085

40. Mercer RE, Michaelson SD, Chee MJS, Atallah TA, Wevrick R, Colmers WF (2013) Magel2 is required for leptin-mediated depolarization of POMC neurons in the hypothalamic arcuate nucleus in mice. PLoS Genet 9(1):e1003207. https://doi.org/10.1371/journal.pgen.1003207

41. Lam DD, Attard CA, Mercer AJ, Myers MG, Rubinstein M, Low MJ (2015) Conditional expression of Pomc in the lepr-positive subpopulation of POMC Neurons is sufficient for normal energy homeostasis and metabolism. Endocrinology 156(4):1292–1302. https://doi.org/10.1210/en.2014-1373

42. Prieur X, Tung YCL, Griffin JL, Farooqi IS, O'Rahilly S, Coll AP (2008) Leptin regulates peripheral lipid metabolism primarily through central effects on food intake. Endocrinology 148(11):5432–5439. https://doi.org/10.1210/en.2008-0498

43. Nogueiras R, Wiedmer P, Perez-Tilve D, et al (2007) The central melanocortin system directly controls peripheral lipid metabolism. J Clin Invest 117(11):3475–3488. https://doi.org/10.1172/JCI31743

44. Klok MD, Jakobsdottir S, Drent ML (2007) The role of leptin and ghrelin in the regulation of food intake and body weight in humans: a review. Obes Rev 8:21–34. https://doi.org/10.1111/j.1467-789X.2006.00270.x

45. Ahima RS (2008) Revisiting leptin's role in obesity and weight loss. J Clin Invest 118:2380–2383. https://doi.org/10.1172/JC136284

46. Coll AP, Farooqi IS, Challis BG, Yeo GSH, O'Rahilly S (2004) Proopiomelanocortin and energy balance: insights from human and murine genetics. J Clin Endocrinol Metab 89:2557–2562. https://doi.org/10.1210/jc.2004-0428

47. Ndisang JF (2010) Role of heme oxygenase in inflammation, insulin-signalling, diabetes and obesity. Mediators Inflamm 2010:1–18. https://doi.org/10.1155/2010/359732

48. Nishimura W, Takahashi S, Yasuda K (2015) MafA is critical for maintenance of the mature beta cell phenotype in mice. Diabetologia 58:566–574. https://doi.org/10.1007/s00125-014-3464-9

49. Butler AE, Robertson RP, Hernandez R, Matveyenko A V., Gurlo T, Butler PC (2012) Beta cell nuclear musculoaponeurotic fibrosarcoma oncogene family A (MafA) is deficient in type 2 diabetes. Diabetologia 55(11):2985–2988. https://doi.org/10.1007/s00125-012-2666-2

50. Guo S, Dai C, Guo M, et al (2013) Inactivation of specific β cell transcription factors in type 2 diabetes. J Clin Invest 123(8):3305–3316. https://doi.org/10.1172/JCI65390